Justin T. Suriano
School of Applied Engineering and Technology,
New Jersey Institute of Technology,
Newark, NJ 07102
e-mail: justin.suriano@njit.edu

Angelantonio Tafuni
Mem. ASME
School of Applied Engineering and Technology,
New Jersey Institute of Technology,
Newark, NJ 07102
e-mail: atafuni@njit.edu

Lewis Mullen
Advanced Technology,
Stryker Orthopaedics,
Mahwah, NJ 07430
e-mail: lewis.mullen@stryker.com

Joseph Racanelli
Advanced Technology,
Stryker Orthopaedics,
Mahwah, NJ 07430
e-mail: joseph.racanelli@stryker.com

Robert Tarantino
Office of the President,
New Jersey Precision Technologies, Inc.,
Mountainside, NJ 07092
e-mail: bob.tarantino@njpt.com

Samuel C. Lieber[1]
Mem. ASME
School of Applied Engineering and Technology,
New Jersey Institute of Technology,
Newark, NJ 07102
e-mail: samuel.lieber@njit.edu

Medical Device Hybrid Manufacturing: Translating the Coordinate System From Metal Additive Manufacturing to Subtractive Post-Processing

Additive manufacturing (AM) has transformed not only how parts can be realized but also their design. Metal additive manufacturing (MAM) has increased AM's utility toward the manufacture of functional products. This has been seen in several industries including medical device, aerospace, and the automotive industries. The main limitation of MAM continues to be the part dimensional tolerances that can be achieved, and the respective surface finish produced. Hybrid manufacturing processes have been used to address these limitations; however, there remain challenges of how to translate the component's coordinate system from AM to subtractive post-processes. This paper explores this topic through a medical device case study. A translatable coordinate system was produced by first designing features to serve as a datum reference frame (DRF). These features were introduced by MAM and then finalized with wire-electrical discharge machining (EDM). The produced DRF features successfully prepared the component for translation from the MAM to subtractive post-process. The completed medical device component met the expected requirements with a less than 1% difference on key part nominal dimensions. In addition, the hybrid process exhibited a potential for sustainable manufacturing with a buy-to-fly ratio of 6:1. The study demonstrated that a coordinate system can be translated effectively in hybrid manufacturing by designing part features informed by both AM and wire-EDM processes. [DOI: 10.1115/1.4062187]

Keywords: additive manufacturing, advanced manufacturing, biomedical manufacturing, computer-aided design, computer-aided manufacturing, design for manufacturing, hybrid processes, manufacturing planning, medical device manufacturing, process engineering

1 Introduction

Additive manufacturing (AM) has transformed not only how we can produce parts but also the process of design. AM, with its reduced setups and fixtures, provides a rapid production of components that has benefited the development of prototypes and evaluation of concepts [1,2]. Metal additive manufacturing (MAM) has opened AM toward the production of functional parts and components. This includes in the medical device, aerospace, and automotive industries [3,4]. There are many advantages to AM where its bottom-up process allows complex features to be created [5], while providing the potential for sustainable manufacturing [6,7]. These advantages can be quantified using simple indices including the buy-to-fly ratio [8–10], which relates the volume of the initial workpiece and the final part. The main limitation of MAM continues to be the respective surface finish that is produced from the grown component [11] as well as tolerances able to be achieved [8]. Hybrid manufacturing processes have been developed to overcome these limitations [3]. These hybrid processes typically integrate AM with subtractive manufacturing (SM) post-processing [8,12–14]. Hybrid manufacturing approaches have included manufacturing equipment with combined additive and subtractive processes [14–16]. These types of systems have now become more commercially available [17]. Researchers have also developed customized process planning software integrated with equipment to address the hybrid approach [13]. These methods show promise; however, the majority of MAM process routes include post-processing with standalone SM [8]. There remains a gap in the literature for hybrid manufacturing process planning utilizing standalone equipment and methods.

The challenge in implementing a hybrid approach with standalone additive and subtractive systems is translating the coordinate system between these two processes [18]. This involves a change in the approach used in the AM digital model design. An AM process alone provides freedom from the implementation of traditional fixtures and tooling [2]. This allows designers to be free from considering coordinate systems in their process planning. In contrast, coordinate system planning is inherent in subtractive manufacturing through the required use of fixtures and tooling. Therefore, the implementation of a successful hybrid manufacturing approach requires the designer to plan for the creation and translation of coordinate systems. This type of approach has been seen in other manufacturing processes, including forgings [19] and castings [20]. Development of process plans with standalone equipment/software allows further integration of MAM as a starting part option in product design. This objective requires addressing the definition and translation of the coordinate system from AM to subtractive processes. Wire electrical discharge machining (EDM) shows promise in facilitating this translation.

[1]Corresponding author.

Manuscript received December 19, 2022; final manuscript received March 14, 2023; published online March 30, 2023. Assoc. Editor: Martin Jun.

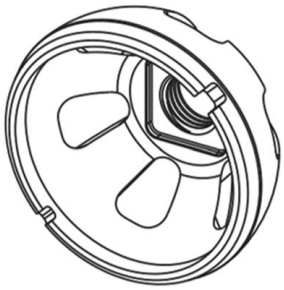

Fig. 1 Sketch of the Stryker Trident Window Trial

A datum reference frame (DRF) is a coordinate system, which can be defined using established standards [21]. ASME Y14.5 [22] is one such standard that provides practices for geometric dimensioning and tolerancing (GD&T) requirements including those for a DRF. The importance of adopting GD&T for components produced by AM alone has been reviewed [23,24]; however, there has been limited discussion on its use in hybrid processes [25,26]. This study begins to address this gap in the literature where we describe how wire EDM shows promise in facilitating this translation.

Wire-EDM is an established technology that has grown in its number of applications in the modern machine shop [27]. The process produces precise geometries and fine surface finishes making it indispensable in several industries including aerospace, medical device, and automotive [28]. The wire-EDM process has been used in the MAM process flow through the removal of parts from build plates [29]. What has not been described in the literature is the use of wire-EDM to produce the datum features on AM parts needed to translate it to a subtractive process. The objective of this work is to explore the use of the wire-EDM platform toward the translation of the coordinate system from the additive to subtractive processes. A medical device case study was selected for this purpose. MAM has been heavily incorporated in the orthopedic medical device industry not only for implants requiring unique foam in-growth features [30] but also in the area of patient-specific custom devices [31,32]. The wire-EDM platform was used to inform the design of the digital file for the MAM starting material. The design of the datum features introduced on the MAM part is also constrained by maximizing the use of standard fixturing in subsequent subtractive machining processes. This work demonstrates a process planning

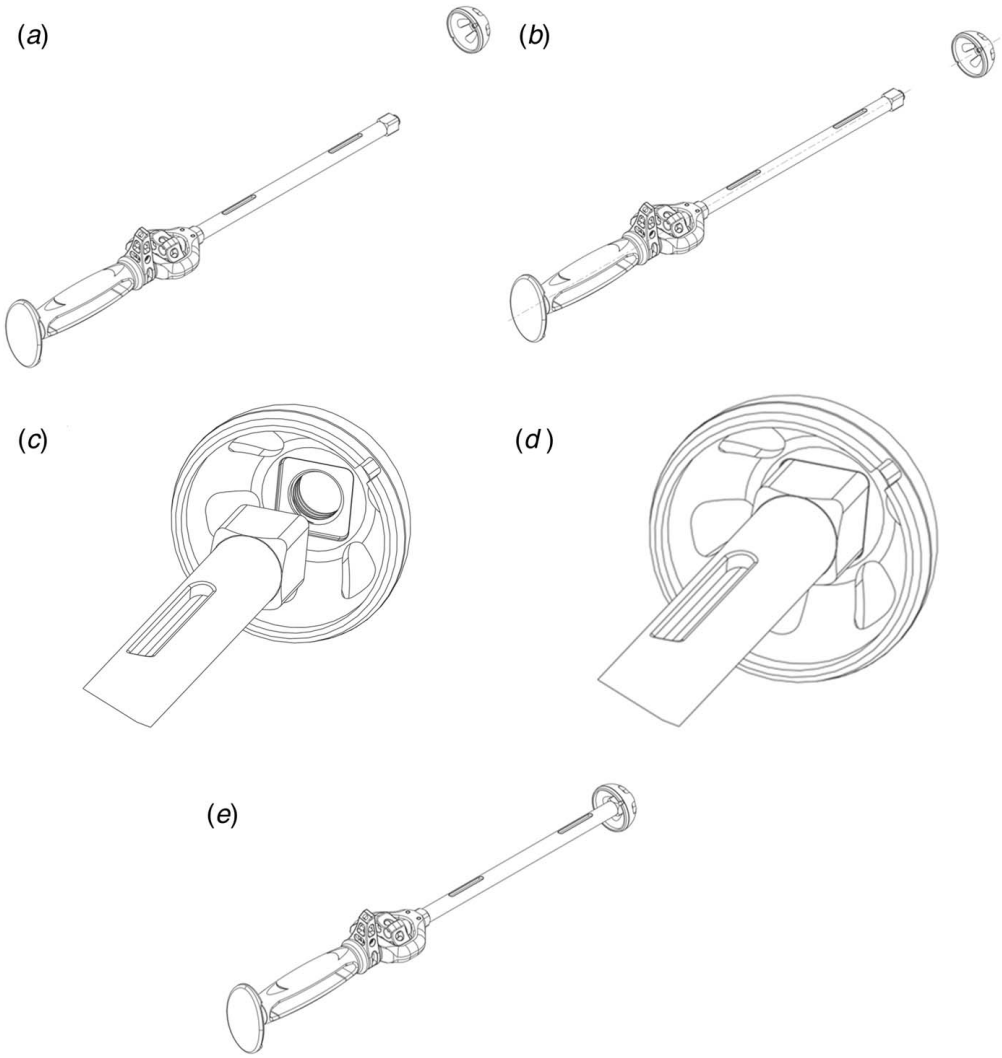

Fig. 2 Assembly of the window trial onto the impactor instrument: (*a*) the window trial is introduced near the impactor, (*b*) the window trial's central axis is aligned to the central axis of the instrument, (c) the window trial square pocket is aligned to the square end of the impactor, (*d*) the impactor is seated on the bottom of the square pocket and threaded in place, and (e) the completed window trial and impactor assembly

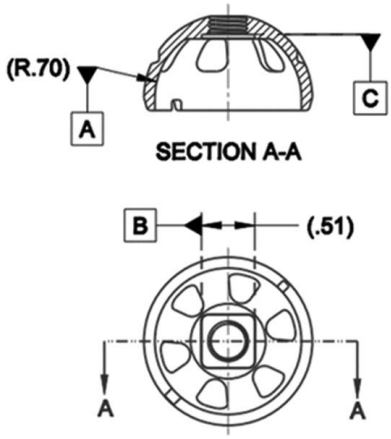

Fig. 3 Trident Window Trial datum features

method that utilizes wire-EDM to introduce a translatable coordinate system for the post-processing of a MAM component.

2 Case Study

2.1 Medical Device. An orthopedic medical device instrument was selected for this hybrid manufacturing study. A component requiring turning, tapping, and milling operations was chosen to fully evaluate the method of translating a coordinate system from the additive to subtractive process. Additionally, a part that is made from stainless steel was chosen to align with the material available in the MAM process at the New Jersey Institute of Technology (NJIT). These criteria led to the selection of the Stryker Orthopaedics' Trident-2 Window Trial Instrument (Fig. 1). The inner and outer radii can be turned, the thread is tapped, and the windows and pocket milled. The Window Trial is used to evaluate the preparation of the acetabulum for the respective acetabular shell, where the windows aid in the fit's visualization [33]. Joint

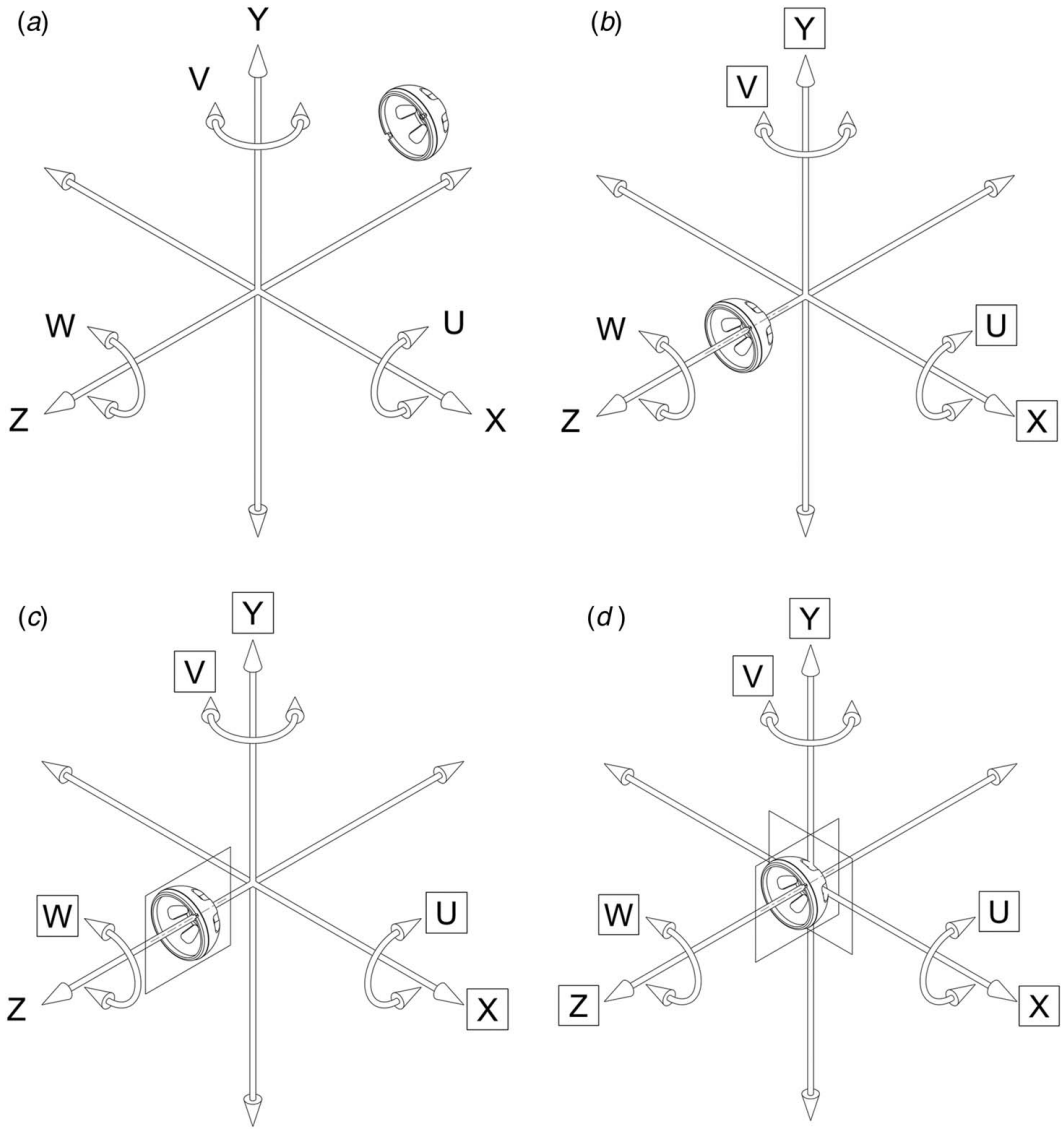

Fig. 4 Representation of how the parts selected datum reference frame constrains the six-degrees of freedom: (*a*) the part is introduced into the coordinate system and no degrees of freedom have been constrained, (*b*) Datum-A, the datum axis, is aligned to the *z*-axis constraining four degrees of freedom, (*c*) Datum-B, the mid-plane, is aligned to the YZ-plane constraining an additional degree of freedom, and (*d*) Datum-C, the plane, is aligned to the XY-plane constraining the final degree of freedom (Degrees of freedom with a box are constrained.)

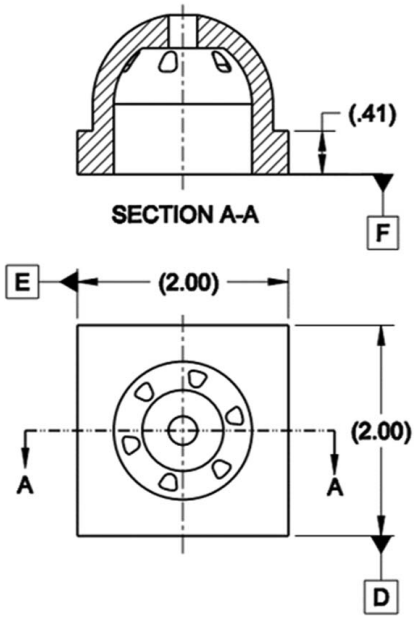

Fig. 5 Additive workpiece datum features

mechanics can also be evaluated with the introduction of a trial insert. The DRF for the component was selected based on its described use [33]. Please note the DRF does not represent what is used by Stryker Orthopaedics and is solely for the purpose of this study.

2.2 Part Datum Reference Frame. The DRF generates a coordinate system on the respective part. This DRF is selected based on the parts function. The manufacturing and inspection process is informed by the DRF. Therefore, the DRF serves to link the manufacture, inspection, and function of the part. The selected part-DRF aligns with the assembly of the window trial onto the impactor instrument (Fig. 2). First, the window trial's central axis is aligned to the central axis of the instrument. Second, the square pocket is aligned to the square end of the impactor. Finally, the impactor is seated on the bottom of the square pocket and threaded in place. This summary of the function informs the datums selected. Figure 3 summarizes the window trial's DRF. The central axis of the window trial will serve as the primary datum (Datum-A). Datum-A can be established through inner radius datum feature of size. The pocket width provides a datum feature of size that produces a mid-plane. This mid-plane will then serve as the secondary datum labeled (Datum-B). The pocket's bottom surface is a datum feature that serves as the tertiary datum (Datum-C). The part-DRF will need to constrain the six-degrees of freedom (6-DOF). Figure 4(*a*) shows the part being introduced into the coordinate system with the 6-DOF. Datum-A, the datum axis, can be aligned to the z-axis (Fig. 4(*b*)), constraining four degrees of freedom. Datum-B, the mid-plane, can be aligned to the YZ-plane (Fig. 4(*c*)), which in turn constrains one degree of freedom. Finally, the plane Datum-C can be aligned to the XY-plane (Fig. 4(*d*)), constraining the final degree of freedom. This part-DRF will be used in the inspection process but also informs the decisions for the DRFs used and produced during the manufacturing process.

3 Additive Workpiece

3.1 Design. The additive workpiece design was informed by the part's final form as well as the additive and post-processing methods selected. The part's final form was determined by reviewing the information provided by Stryker Orthopaedics. This included the nominal size of the features, confidential tolerance requirements, and an as-machined surface finish requirement. Please note the as-machined surface finish was selected for the purposes of this study and does not represent the Stryker production-part. The additive process was driven by the experience with the EOS M280 unit at NJIT. The post-processing methods were constrained to wire-EDM, CNC-milling, and CNC-turning available at New Jersey Precision Technology (NJPT). The additive workpiece design involved starting with the part's final form and modifying it to address the additive and subtractive manufacturing processes. A nominal-sized CAD model was provided by Stryker Orthopaedics as a starting point for the additive workpiece. The MAM process produces a part with a rough surface finish [11] and high dimensional tolerance grade [8]. Features were therefore oversized/undersized by 0.047 in. in order to account for the post-process machining needed to achieve the part's final form. The 0.047 in. was based on the NJPT's experience post-processing MAM components. Features that were smaller than, or near the oversize/undersize value were removed from the CAD model. This included the square cut out with a nominal depth of 0.043 in., the grooves on the top of the cup, as well as all rounds and chamfers. The 3/8-24 tapped hole at the top of the dome was sized based on common drill sizes. The typical drill size for the 3/8-24 tap would be a Q (0.3320 in.) letter size drill. The hole was sized to an I drill (0.2720 in.) to then be enlarged for the eventual tapping operation. A sacrificial square flange (Fig. 5) was introduced to locate and clamp the additive workpiece for the subtractive post-processing. The square flange is oriented in the same direction as the square pocket on the window trial. This orients the windows, which are additively introduced and will be enlarged during the subtractive process. To accommodate the sacrificial square flange, the window trial rim was oversized axially by the 0.047 in. and an additional 3/32 in. to accommodate lathe tooling to post-process the outer diameter. A square flange shape was selected because it allows the additive workpiece to be held with off-the-shelf workholding, can be prepared with the wire-EDM process, and provides a foundation for the DRF. This reference frame could then be used to transfer the additive coordinate system to the subtractive post-process.

3.2 Additive Datum Reference Frame. The additive-DRF translates the coordinate system from the additive process to the subtractive one. The additive-DRF aligns with the part-DRF and similarly constrains the six DOFs. The sacrificial square flange provides datum features that can be first prepared additively and then finalized with the wired-EDM process. The 3–2–1 principle was used to define a set of three mutually perpendicular features (planes and mid-planes) for the additive-DRF (Fig. 5). The square flange has two features of size that generates mid-planes. A mid-plane (Datum-D) is generated from the size of one set of the flange's parallel surface and another (Datum-E) from the other. The final datum feature (Datum-F) is generated during the removal of the part from the build plate through the wire-EDM process. The additive-DRF constrains the six-degrees of freedom (6-DOF). Figure 6(*a*) shows the additive workpiece being introduced into the coordinate system with the 6-DOF. Datum-D, the mid-plane, is aligned to the YZ-plane. This constrains three degrees of freedom (Fig. 6(*b*)). Datum-E, the mid-plane, can be aligned to the XZ-plane. This datum plane in turn constrains two degrees of freedom (Fig. 6(*c*)). Finally, Datum-F, the plane, can be aligned to the XY-plane constraining the final degree of freedom (Fig. 6(*d*)).

4 Hybrid Manufacturing Process

The additive and subtractive process steps are independent of the current production process used by Stryker Orthopaedics and were developed for the purpose of this study. The window trial was

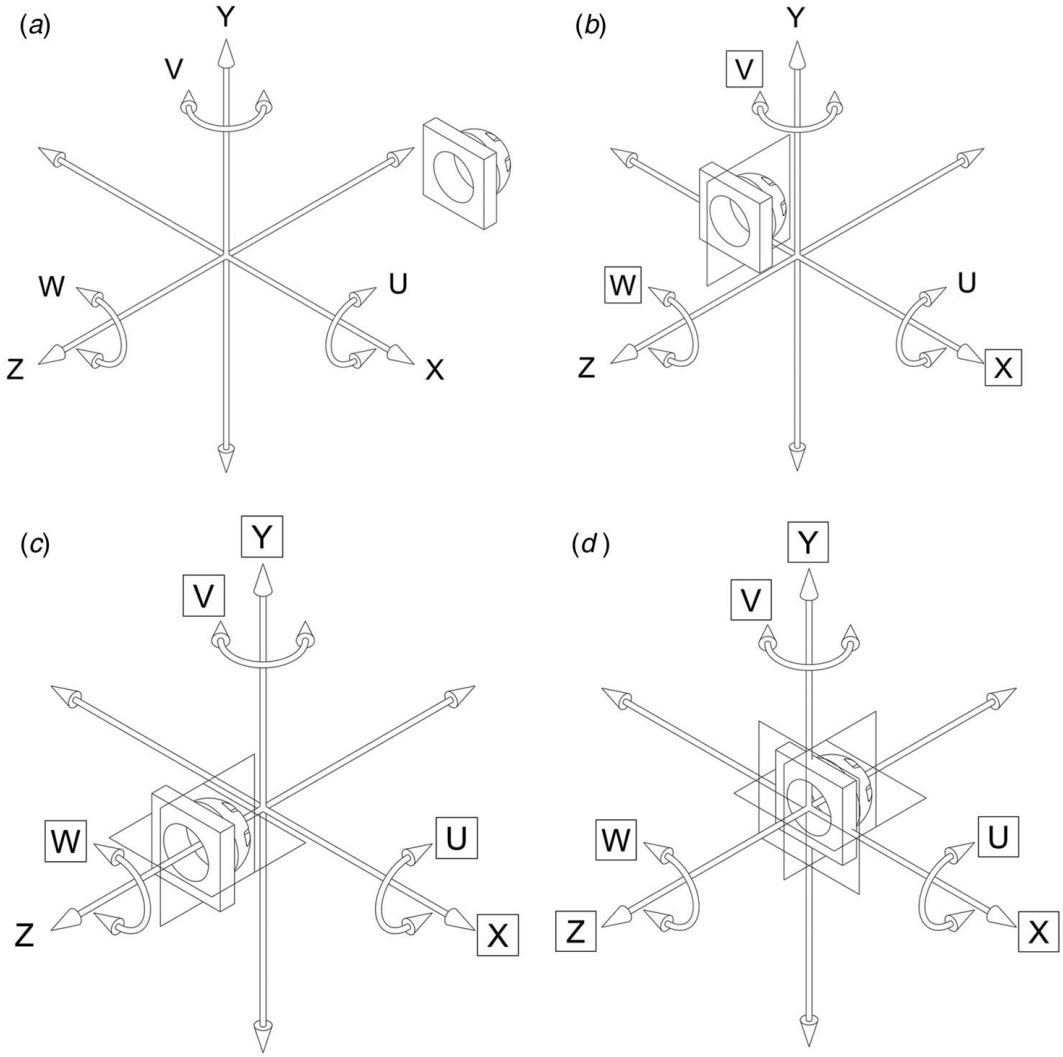

Fig. 6 Representation of how the additive workpiece selected datum reference frame constrains the six-degrees of freedom: (*a*) the additive workpiece is introduced into the coordinate system and no degrees of freedom have been constrained, (*b*) Datum-D, the mid-plane, is aligned to the YZ-plane constraining three degrees of freedom, (*c*) Datum-E, the mid-plane, is aligned to the XZ-plane constraining an additional two degrees of freedom, and (*d*) Datum-F, the plane, is aligned to the XY-plane constraining the final degree of freedom. (Degrees of freedom with a box are constrained.)

produced through a series of eight operations. Materialise MAGICS 23 was used to prepare the additive workpiece for the MAM process. MasterCAM Version 2020-Curve/Drill/5Axis was used to prepare the code for the CNC machining process.

Operation-1. The additive workpiece was grown at the NJIT MakerSpace using the EOS M280 additive metal manufacturing system fitted with a 200W Yb fiber laser. The parts were printed in a nitrogen atmosphere produced by a nitrogen generator attached to the EOS M280. EOS PH1 metal powder was used to print the test artifacts with a 20 μm layer thickness. EOS described that the PH1 powder is related to 15-5 PH stainless steel [34]. The parts were printed on a 420 stainless steel build plate meeting EOS surface roughness and geometric specifications. Figure 7 shows a cross-section CAD image of the AM supports, and the representative image of the additive workpiece on the build plate.

Operation-2. The build plate with the additive workpiece was loaded onto a Mitsubishi Model FA20S Advance Wire-Electrical Discharge Machine (EDM). The build plate was oriented such that its largest surface was parallel to the 0.012-in. diameter brass wire. The build plate surface was located and indicated. A 1-in. gauge block was then used to locate and indicate the square flange edge (Fig. 8(*a*)). The wire was then used to remove 0.015 in off both parallel surfaces that define the mid-plane Datum-D (Figs. 8(*b*)–8(*c*)).

Operation-3. The build plate with the additive workpiece from Operation-1 was then rotated ninety degrees and fixed in the wire EDM unit. The build plate's largest surface was oriented such that it was parallel to the EDM's wire. The build plate surface

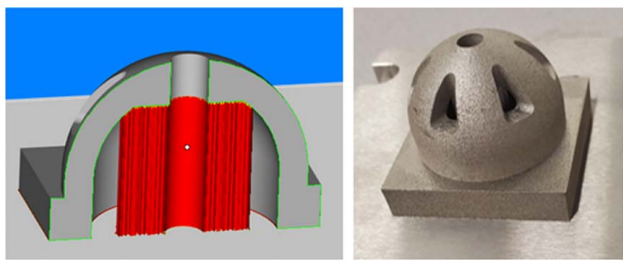

Fig. 7 Metal additive manufacturing operation. Supports are generated in the MAGICS software to support the component's dome (left). The additive workpiece is shown fused to the build plate after a completed additive manufacturing run (right).

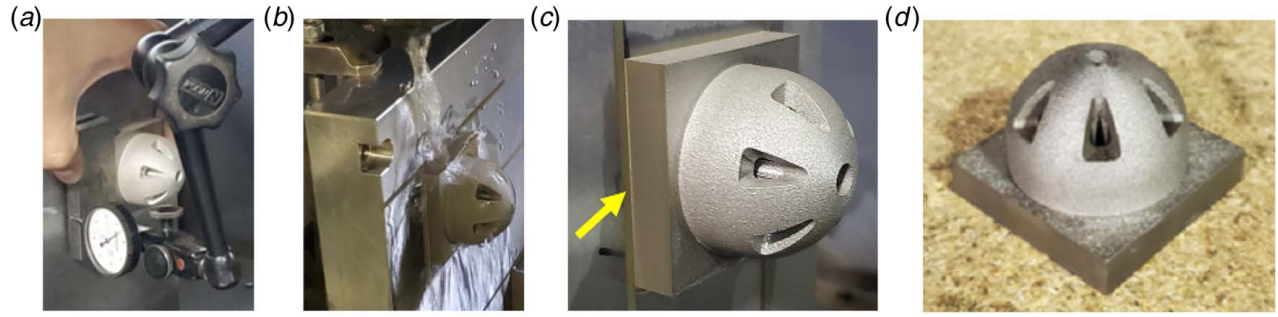

Fig. 8 The wire EDM process: (*a*) 1-in. gauge block used to locate and indicate the square flange edge, (*b*) wire-EDM cutting datum feature, (c) arrow points to flange side that was cut by wire-EDM, and (*d*) additive workpiece fully prepared on wire-EDM

was located and indicated. The flange edges were again located and indicated. The wire was then used to remove 0.015 in off both parallel surfaces that define the mid-plane of Datum-E (Figs. 8(*b*)–8(*c*)). The wire picked up the surface of the build plate and subsequently cut the part off the build plate producing Datum-F. The additive workpiece that was removed from the build plate is shown in Fig. 8(*d*).

Operation-4. A Haas CNC Turning Center (Model ST15) was used to remove the additive supports and prepare the inner radius. A four-jaw chuck was outfitted with machined jaws that serve as datum simulators for datum features D and E (Fig. 9(*a*)). Solid carbide tool inserts were used for the operation. The workpiece's flange was located and indicated to establish the work and tool offsets needed for the CNC program. The workpiece post-machining is shown in Fig. 9(*b*) with the supports removed and the inner surface machined.

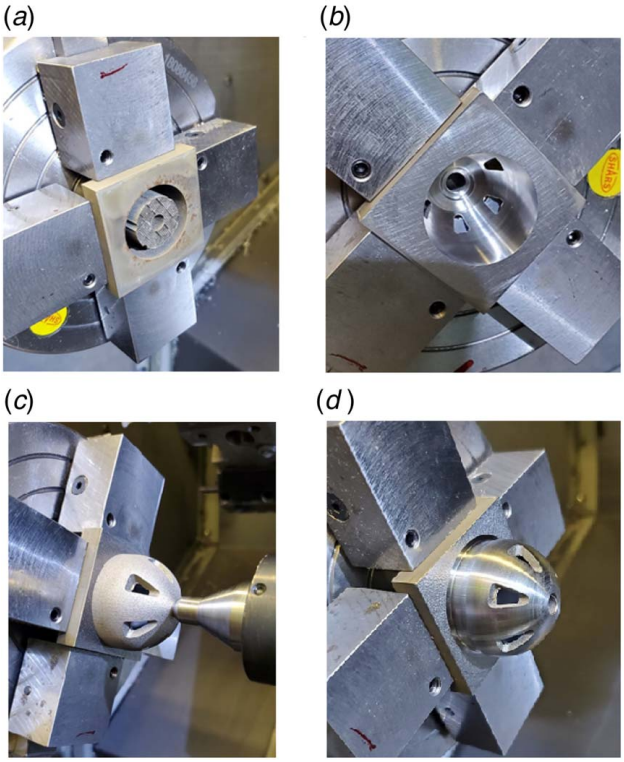

Fig. 9 CNC turning operations: (*a*) the workpiece located and clamped in the four-jaw chuck with machined jaws serving as datum simulators, (*b*) additive workpiece post-machining with additive supports removed and inner surface machined, (*c*) the additive workpiece is rotated, located, and clamped in the turning centers four jaws. A support is used through the additive clearance hole to support during turning, and (*d*) additive workpiece post-machining with outer surface machined.

Operation-5. The Haas CNC Turning Center (Model ST15) was then used to prepare the outer radius. The workpiece was rotated and the same four-jaw chuck with the machined jaws used in Operation 4 served as datum simulators for datum features D and E (Fig. 9(*c*)). Solid carbide tool inserts were also used for the operation. Additional support is provided with a tailstock that references the grown through hole on the dome. This was needed because of the interrupted cut generated from the additively introduced windows. The outside on the Window trial was turned (Fig. 9(*d*)) and then removed from the CNC turning center.

Operation-6. A Haas CNC Mill (Model VF2SS) was then used to mill the windows. A Kurt vise with standard parallels was used as datum simulators for both datum features D and F (Fig. 10(*a*)). Datum feature E was located to establish the datum reference frame for milling the windows. A 3/16-in. diameter end mill was used for the roughing and finishing. Figure 10(*b*) shows the additive workpiece post-machining with the windows machined to size.

Operation-7. The workpiece was then rotated and reinstalled in the Haas CNC Mill (Model VF2SS) with the Kurt vise and standard parallels serving as datum simulators for datum features D and F (Fig. 10(*c*)). Datum feature E was located to establish the datum reference frame for milling the pocket. An 1/8-in. diameter flat endmill was used to prepare the square pocket. The preparation of the pocket is datum features B and C in the window trial. The existing hole then was enlarged with the 1/8-in. endmill, chamfered with a 1/4-in. diameter chamfer end mill, and then tapped (Fig. 10(*d*)).

Operation-8. The workpiece was then installed into a fixture that provided support to the workpiece's outer radius. The workpiece was then fastened into the fixture utilizing the tapped hole. The square flange was also supported (Fig. 11(*a*)). The workpiece was then located and the Haas CNC Mill (Model VF2SS) was then used to sever the square flange with a 3/8-in. flat end mill (Fig. 11(*b*)). The clamps were removed along with the supported flange remnant (Fig. 11(*c*)). The workpiece was then finished with ball and chamfer endmills to produce the chamfer, rounds, and grooves (Fig. 11(*d*)).

Evaluation. A Zeiss CMM (Model Contura G2 7/10/6 RDS with Zeiss VAST XXT probe) was used to conduct geometric measurements (Fig. 12). This included the inner and outer spherical radii, the position of the windows, and the position of 3/8-24 tapped hole. These measures were done with reference to the DRF described in Fig. 3. The overall height (Fig. 12) of the component was also measured with a Mitutoyo model HDS-H12"C Digimatic height gage. The inner and outer spherical radii, and overall height are key features that interact with mating parts. They were also measured on a Stryker Orthopaedics' released production-part for comparison.

5 Evaluation and Discussion

The hybrid process plan was successfully executed producing the completed window trial (Fig. 13). The wire-EDM prepared sacrificial flange facilitated the transfer of the coordinate system from the

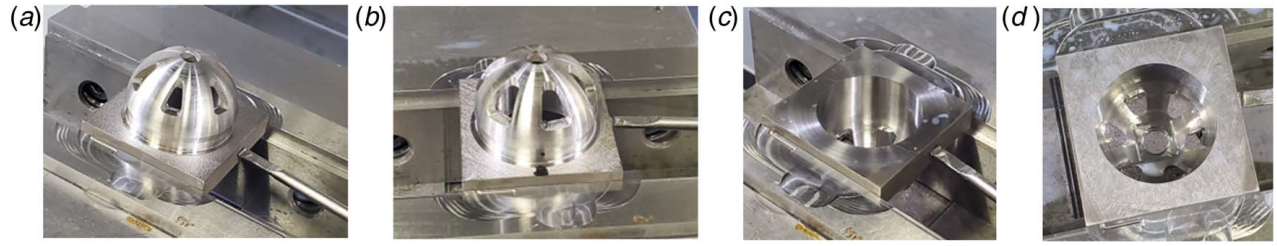

Fig. 10 Milling operations: (*a*) the workpiece located and clamped in a Kurt vise with parallels that serve as datum simulators, (*b*) additive workpiece post-machining with the windows machined to size, (*c*) the additive workpiece is rotated, located, and clamped in the Kurt vise with parallels which serve as datum simulators, and (*d*) the square pocket is machined and the dome's hole opened up for a 3/8-24 tap

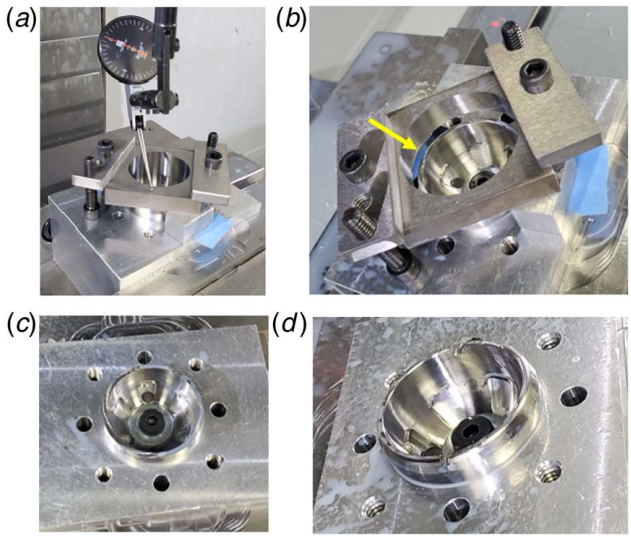

Fig. 11 Milling operations to remove flange and complete part: (*a*) the workpiece was located and clamped in fixture that provided support to the workpiece's outer radius, supported and clamped the flange, and allowed the workpiece to be fastened to the fixture through the tapped hole, (*b*) the arrow shows the region where the square flange was severed, (*c*) the clamps were removed along with the supported flange remnant, and (*d*) The workpiece was then finished with chamfer, rounds, and grooves

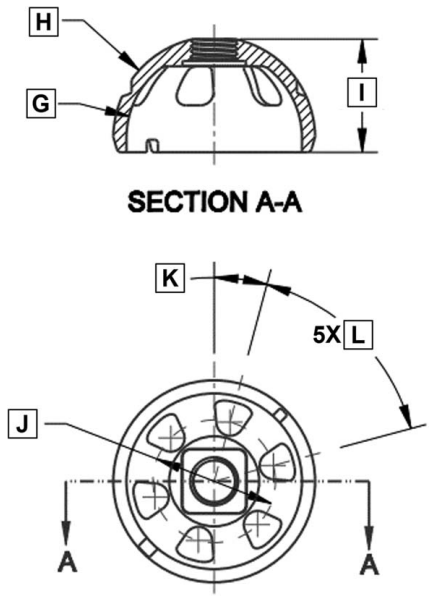

Fig. 12 Evaluation measures conducted on completed window trial. G and H are the inner outer spherical radii, respectively. I is the overall height of the component. J, K, and L provide the positional information for the windows.

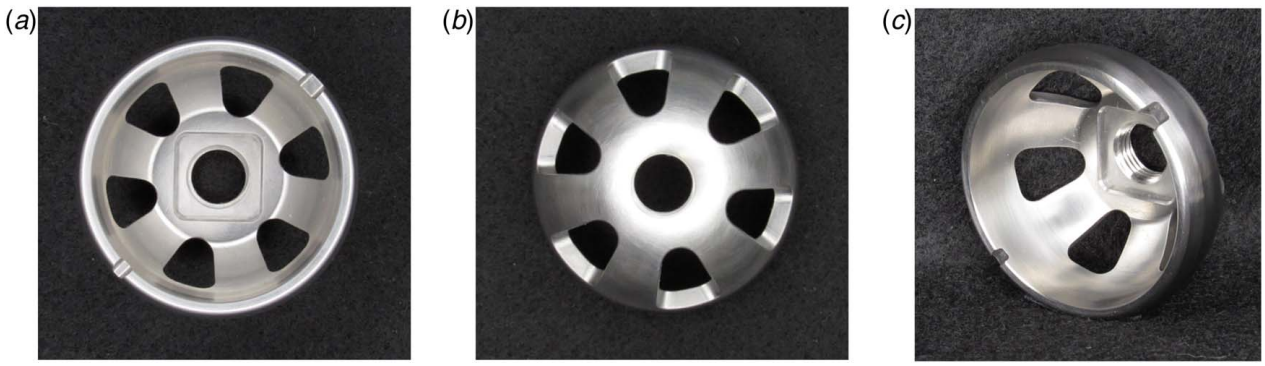

Fig. 13 A completed window trial: (*a*) view inside the window trial where the square pocket is visible, (*b*) view from the top of the window trial's dome, and (*c*) three-dimensional view of completed window trial.

AM process to the SM post-process. This allowed the near net shaped features to be located and machined to size. The flange's wire-EDM prepared surface also allowed the use of standard workholding for the majority of the process steps (Operations 1–7). The lone exception, Operation 8, involved a fixture that supported the component's outer radius toward severing the flange and finishing the component. The use of standard workholding for this step could be explored in the future. The reduction of custom fixturing presents a unique advantage of introducing a flange feature in the additively grown part. This geometry coupled with the wire-EDM

Table 1 The percentage difference between the measured and CAD nominal dimension for this study's hybrid component and a production-part

Part dimension	Hybrid component measured to nominal (% difference)	Production-part measured to nominal (% difference)
G	0.29	0.20
H	0.40	0.21
I	0.77	0.18
J	0.03	–
K	0.73	–
L	0.04	–

surface preparation makes the flange structure able to be clamped withstanding the loads seen during the turning and milling processes. Thus, the wire-EDM prepared flange serves not only to translate the respective manufacturing coordinate system but also as a feature to facilitate the use of off-the-shelf workholding. This highlights the potential of AM to support sustainable manufacturing through the reduction of fixtures [7,35]. Another index of sustainable manufacturing used in AM/SM comparisons is the buy-to-fly ratio [8–10]. In this study, the final part's buy-to-fly ratio was estimated from the respective CAD models to be 6:1. This is an improvement over a subtractive alone buy-to-fly ratio of 38:1, which was estimated from a round billet starting material (2-in. diameter by 4-in. length). In addition, the 6:1 ratio is in alignment with aerospace ratios that have been reported as 10:1 from parts machined out of die forgings, hand forgings, or plate stock [9]. The observed machinability of the additive starting material was similar to what has been seen with a standard billet processed in a subtractive alone process. This experience has also been found with turning and milling of other SLM produced metals, as reviewed in Ref. [36]. A full study would need to be conducted to quantify the observed machinability. The only machining concern was the potential increased tool wear that could result from the interrupted cuts (Operations 4–5). Further studies would have to be conducted to evaluate if the sustainability benefit of the windows in the additive workpiece outweighs the potential tool wear introduced with the interrupted cut. The surface finish was also achieved with the same processing and parameters that would be used on a billet in a subtractive alone operation. The completed part machined to an as-machined surface finish. This finding is also consistent with other work describing the fine surface finishes achieved through CNC machining of MAM material [37]. The inspection demonstrated a less than 1% difference when comparing the part measures to the CAD model nominal values (Table 1). This included the inner (G) and outer (H) radii of the window trial that were oversized in the additive model. These features post-machining were 0.29% and 0.40% different than their nominal values, respectively. The removal of the sacrificial flange and preparation of the final height of the component also proved effective. The overall height of the component (I) was 0.77% different than the nominal measure. The radii along with the overall height are key features that interact with mating parts. They provide insight into whether the developed hybrid process could eventually be interchangeable with a subtractive one. The hybrid component measures were in the range of, but higher than those conducted on the established production-part (Table 1). This includes the overall height, which points to the potential need for improvement in the flange removal process. The hybrid process; however, still demonstrated promise toward being interchangeable with the subtractive one. The 3/8-24 tapped hole and windows were undersized on the additive workpiece. The position of the 3/8-24 tapped hole on the produced part was less than 0.001 in. from the CAD nominal value. In addition, the window pattern circle (J) was 0.03% different than nominal and the angular position to the first window (K) and each window (L) was 0.73% and 0.04%, respectively. In summary, these differences were viewed as acceptable by Stryker Orthopaedics for a prototype process that has yet to be optimized.

This study demonstrates that coordinate system translation planning should be considered in a hybrid manufacturing process. Leaving the AM starting material at near net shape with no identifiable datum features presents large challenges for the eventual subtractive post-processing [18]. Datum features should be considered during the digital design phase in order to facilitate the transfer of the AM component to the subsequent SM post-process. This approach is also consistent with other near net shape starting workpiece processes. This includes castings [38] which have a strong similarity to the process considerations done with AM parts. Although the square flange in this case study proved to be effective it does not mean it is the only approach. Future work on this type of feature includes exploring whether the flange size could be minimized or hollowed to reduce the additive material used. In addition, exploration is needed on the geometry and its location on the additive workpiece. The effectiveness of this type of feature would need to be further explored with not only geometric but also freeform shapes. A square flange introduced on one end of a freeform shape is expected to support coordinate translation and the use of standard workholding; however, may not be sustainable. The use of datum targets [23] in conjunction with other robust clamping features may provide the best solution. This future work should be conducted on an established [39] or developed test artifact. This would allow the reporting of dimensions, tolerances, and comparisons to other published work. In addition, an optimal test artifact shape should be chosen that allows for the cost-effective preparation of the number of samples needed to conduct statistical comparisons. This would enable evaluating the effectiveness of the coordinate system translation solution in overcoming the dimensional and mechanical property variability that exists in a MAM process [40]. Future solutions would have to balance the needs of sustainable manufacturing, defining a translatable DRF, and the ability of the part to be secured in workholding during the machining process. Regardless of the design of the additive feature supporting the DRF, wire-EDM should be considered as the platform to prepare the DRF on the additively produced part. This is anticipated to be effective on most MAM systems on the market [40], including powder bed fusion (PBF) and direct energy deposition (DED) technologies. DED potentially could provide increased sustainable options, where the DED-substrate could replace additively grown features used for coordinate system translation and fixturing. An alternative process to wire-EDM would need to be explored if the selected AM process produces nonconductive components.

6 Conclusions

MAM has reshaped the way products can be realized with its ability to produce unique features only achievable through an additive approach. The current limitations in MAM (e.g., surface finish) require a post-processing method. SM has proven itself to be a highly effective means to post-process MAM components. This option requires the designer to keep in mind how to translate coordinate systems from the AM to SM. This study demonstrated the effective use of wire-EDM to establish a DRF on an additive workpiece. This prepared surface allowed for the use of standard workholding towards the post-process machining of the component. The findings of this study suggest that when design for AM considers post-process machining, features should also be introduced to establish a DRF. This approach, however, may eventually be unnecessary with the potential successful implementation of post-processing of additive components with mass media finishing [41].

Acknowledgment

The authors would like to thank the team at New Jersey Precision Technologies, Inc. for all their support, especially the efforts of Laurie Bertolotti and Michal Obloj. The authors would also like

to thank Matthew Demers at Stryker Orthopaedics for his product development support.

Funding Data

- Stryker Orthpaedics provided funding for the purchase of supplies used for the Metal Additive Manufacturing process.

Notes

All figures used in this manuscript are representative.

Conflict of Interest

Robert Tarantino was an employee of New Jersey Precision Technologies, Inc. during the work conducted for this manuscript. Joseph Racanelli and Lewis Mullen were employees of Stryker Orthopaedics during the work conducted for this manuscript. No other author has a financial interest/personal relationship which may be considered as potential competing interests.

Data Availability Statement

The datasets generated and supporting the findings of this article are obtainable from the corresponding author upon reasonable request.

References

[1] Negi, S., Dhiman, S., and Sharma, R. K., 2013, "Basics, Applications and Future of Additive Manufacturing Technologies: A Review," J. Manuf. Technol. Res., **5**(1/2), pp. 75–96.

[2] Beaman, J. J., Bourell, D. L., Seepersad, C. C., and Kovar, D., 2020, "Additive Manufacturing Review: Early Past to Current Practice," ASME J. Manuf. Sci. Eng., **142**(11), p. 110812.

[3] Abdulhameed, O., Al-Ahmari, A., Ameen, W., and Mian, S. H., 2019, "Additive Manufacturing: Challenges, Trends, and Applications," Adv. Mech. Eng., **11**(2), p. 1687814018822880.

[4] Bahnini, I., Rivette, M., Rechia, A., Siadat, A., and Elmesbahi, A., 2018, "Additive Manufacturing Technology: the Status, Applications, and Prospects," Int. J. Adv. Manuf. Technol., **97**(1), pp. 147–161.

[5] Tofail, S. A., Koumoulos, E. P., Bandyopadhyay, A., Bose, S., O'Donoghue, L., and Charitidis, C., 2018, "Additive Manufacturing: Scientific and Technological Challenges, Market Uptake and Opportunities," Mater. Today, **21**(1), pp. 22–37.

[6] Mehrpouya, M., Dehghanghadikolaei, A., Fotovvati, B., Vosooghnia, A., Emamian, S. S., and Gisario, A., 2019, "The Potential of Additive Manufacturing in the Smart Factory Industrial 4.0: A Review," Appl. Sci., **9**(18), p. 3865.

[7] Javaid, M., Haleem, A., Singh, R. P., Suman, R., and Rab, S., 2021, "Role of Additive Manufacturing Applications Towards Environmental Sustainability," Adv. Ind. Eng. Polym. Res., **4**(4), pp. 312–322.

[8] Pragana, J., Sampaio, R., Bragança, I., Silva, C., and Martins, P., 2021, "Hybrid Metal Additive Manufacturing: A State–of–the-art Review," Adv. Ind. Manuf. Eng., **2**, p. 100032.

[9] Kobryn, P. A., Ontko, N. R., Perkins, L. P., and Tiley, J. S., 2006, "Additive Manufacturing of Aerospace Alloys for Aircraft Structures," Cost Effect. Manuf. Net-Shape Process., **139**(3), pp. 1–14.

[10] Watson, J. K., and Taminger, K. M. B., 2018, "A Decision-support Model for Selecting Additive Manufacturing Versus Subtractive Manufacturing Based on Energy Consumption," J. Cleaner Prod., **176**, pp. 1316–1322.

[11] Lee, J.-Y., Nagalingam, A. P., and Yeo, S. H., 2021, "A Review on the State-of-the-art of Surface Finishing Processes and Related Iso/astm Standards for Metal Additive Manufactured Components," Virtual Phys. Prototyping, **16**(1), pp. 68–96.

[12] Popov, Vladimir V., and Fleisher, Alexander, 2020, "Hybrid Additive Manufacturing of Steels and Alloys," Manuf. Rev., **7**, p. 6.

[13] Manogharan, G., Wysk, R., Harrysson, O., and Aman, R., 2015, "Aims – a Metal Additive-hybrid Manufacturing System: System Architecture and Attributes," Procedia Manuf., **1**, pp. 273–286.

[14] Flynn, J. M., Shokrani, A., Newman, S. T., and Dhokia, V., 2016, "Hybrid Additive and Subtractive Machine Tools – Research and Industrial Developments," Int. J. Mach. Tools Manuf., **101**, pp. 79–101.

[15] Sefene, E. M., Hailu, Y. M., and Tsegaw, A. A., 2022, "Metal Hybrid Additive Manufacturing: State-of-the-art," Progr. Addit. Manuf., **7**(4), pp. 737–749.

[16] Lalegani Dezaki, M., Serjouei, A., Zolfagharian, A., Fotouhi, M., Moradi, M., Ariffin, M., and Bodaghi, M., 2022, "A Review on Additive/subtractive Hybrid Manufacturing of Directed Energy Deposition (DED) Process," Adv. Powder Mater., **1**(4), p. 100054.

[17] Saunders, S., 2021, "Hybrid 3D Printing Tech Developed by Phillips Corp., Haas, & Meltio," Online Article, 3Dprint.com, Aug. 18.

[18] Hider, J., 2022, "An Additive Manufacturing Machine Shop," Online Article, mmsonline.com, Nov. 19.

[19] Caporalli, A., Gileno, L. A., and Button, S. T., 1998, "Expert System for Hot Forging Design," J. Mater. Process. Technol., **80–81**, pp. 131–135.

[20] Pattnaik, S., Karunakar, D. B., and Jha, P., 2012, "Developments in Investment Casting Process–a Review," J. Mater. Process. Technol., **212**(11), pp. 2332–2348.

[21] Wu, Y., and Gu, Q., 2016, "The Composition Principle of the Datum Reference Frame," Procedia CIRP, **43**, pp. 226–231. 14th CIRP CAT 2016 – CIRP Conference on Computer Aided Tolerancing.

[22] ASME, 2019, *Y14.5-1994, 1995, Dimensioning and Tolerancing*, ASME, New York.

[23] Vakouftsis, C., Mavridis-Tourgelis, A., Kaisarlis, G., Provatidis, C. G., and Spitas, V., 2020, "Effect of Datum System and Datum Hierarchy on the Design of Functional Components Produced by Additive Manufacturing: a Systematic Review and Analysis," Int. J. Adv. Manuf. Technol., **111**(3), pp. 817–828.

[24] Pei, E., Kabir, I., Breški, T., Godec, D., and Nordin, A., 2022, "A Review of Geometric Dimensioning and Tolerancing (GD&T) of Additive Manufacturing and Powder Bed Fusion Lattices," Progr. Addit. Manuf., **7**(6), pp. 1297–1305.

[25] Ameta, G., Lipman, R., Moylan, S., and Witherell, P., 2015, "Investigating the Role of Geometric Dimensioning and Tolerancing in Additive Manufacturing," ASME J. Mech. Des., **137**(11), p. 111401.

[26] Ameta, G., Moylan, S., Witherell, P., and Lipman, R., 2015, "Challenges in Tolerance Transfer for Additive Manufacturing," Proceedings – ASPE 2015 Spring Topical Meeting: Achieving Precision Tolerances in Additive Manufacturing, Raleigh, NC, Apr. 26–29, Vol. 1, pp. 129–135.

[27] Slătineanu, L., Dodun, O., Coteaţă, M., Nagîţ, G., Băncescu, I. B., and Hriţuc, A., 2020, "Wire Electrical Discharge Machining—A Review," Machines, **8**(4), p. 69.

[28] Li, L., Guo, Y., Wei, X., and Li, W., 2013, "Surface Integrity Characteristics in Wire-EDM of Inconel 718 At Different Discharge Energy," Procedia CIRP, **6**, pp. 220–225. Proceedings of the Seventeenth CIRP Conference on Electro Physical and Chemical Machining (ISEM).

[29] Hider, J., 2020, "Cutting AM Parts From Build Plate Turns Wire EDM Upside Down," Online Article, mmsonline.com, Dec. 17.

[30] Dall'Ava, L., Hothi, H., Di Laura, A., Henckel, J., and Hart, A., 2019, "3d Printed Acetabular Cups for Total Hip Arthroplasty: A Review Article," Metals, **9**(7), p. 729.

[31] Bastin, A., and Huang, X., 2022, "Progress of Additive Manufacturing Technology and Its Medical Applications," ASME Open J. Eng., **1**, p. 010802.

[32] Murr, L. E., 2020, "Global Trends in the Development of Complex, Personalized, Biomedical, Surgical Implant Devices Using 3d Printing/additive Manufacturing: A Review," Med. Devices Sens., **3**(6), p. e10126.

[33] Stryker, 2020, "Trident II Tritanium Acetabular System Surgical Protocol," TRITRI-SP-2_Rev-5_23300, pp. 1–32.

[34] Croccolo, D., De Agostinis, M., Fini, S., Olmi, G., Bogojevic, N., and Ciric-Kostic, S., 2018, "Effects of Build Orientation and Thickness of Allowance on the Fatigue Behaviour of 15–5 Ph Stainless Steel Manufactured by Dmls," Fatigue Fract. Eng. Mater. Struct., **41**(4), pp. 900–916.

[35] Mani, M., Lyons, K., and Gupta, S., 2014, "Sustainability Characterization for Additive Manufacturing," J. Res. Natl. Inst. Stand. Technol., **119**, pp. 419–428.

[36] Uçak, N., Çiçek, A., and Aslantas, K., 2022, "Machinability of 3d Printed Metallic Materials Fabricated by Selective Laser Melting and Electron Beam Melting: A Review," J. Manuf. Process., **80**, pp. 414–457.

[37] Simoni, F., Huxol, A., and Villmer, F.-J., 2021, "Improving Surface Quality in Selective Laser Melting Based Tool Making," J. Intell. Manuf., **32**, pp. 1927–1938.

[38] Jiayi, W., Sama, S. R., and Manogharan, G., 2019, "Re-Thinking Design Methodology for Castings: 3D Sand-Printing and Topology Optimization," Int. J. Metalcast., **13**, pp. 2–17.

[39] Moylan, S., Slotwinski, J., Cooke, A., Jurrens, K., and Donmez, M. A., 2014, "An Additive Manufacturing Test Artifact," J. Res. Natl. Inst. Stand. Technol., **119**, pp. 429–459.

[40] Vafadar, A., Guzzomi, F., Rassau, A., and Hayward, K., 2021, "Advances in Metal Additive Manufacturing: A Review of Common Processes, Industrial Applications, and Current Challenges," Appl. Sci., **11**(3), p. 1213.

[41] Boschetto, A., Bottini, L., Macera, L., and Veniali, F., 2020, "Post-Processing of Complex Slm Parts by Barrel Finishing," Appl. Sci., **10**(4), p. 1382.